Autofocusing of Optical Scanning Holography Based on Entropy Minimization

Zhenbo Ren, Ni Chen, Antony Chan, Edmund Lam*

Imaging Systems Laboratory, Department of Electrical and Electronic Engineering, The University of Hong Kong, Pokfulam Road, Hong Kong

**elam@eee.hku.hk*

Abstract: In optical scanning holography, extracting distance of object is an indispensable step for numerical reconstruction. In this paper, we use entropy as a measurement to achieve autofocusing under different situations.

OCIS codes: 090.1760, 100.3010.

1. Introduction

Optical scanning holography (OSH) is a form of incoherent digital holography [1]. It can be used to record three-dimensional (3D) object in a two-dimensional (2D) hologram with active scanning and heterodyne demodulation. After the lateral scanning, a digital hologram is available in the computer to reconstruct different sections of the real 3D object numerically. This technique has been applied to many areas, such as microscopy [2], and remote sensing [3].

In the reconstruction process, a key step is to establish the Fresnel zone plate (FZP), which is related to the distance between each section of the object and the photodetector. Various methods have been developed to deal with the autofocusing problem, along with identifying how many sections that the hologram records [4–6]. Here we propose a new method based on entropy minimization to achieve autofocusing in OSH. This technique is verified by simulations under different situations.

2. OSH Model and Mathematical Principles

Essentially, OSH is a linear space-invariant optical imaging system for a specific axial distance. A 3D object is located at a distance of z to the active scanner. A photodetector behind the object collects the wavefront of interference pattern which carries the information of the object. With the help of heterodyne detection, a hologram can be recorded digitally, which makes numerical reconstruction of different sections possible. Fig. 1a is the basic architecture of the OSH system, and Fig. 1b and 1c show the two hollow objects we will use in the consequent simulations.

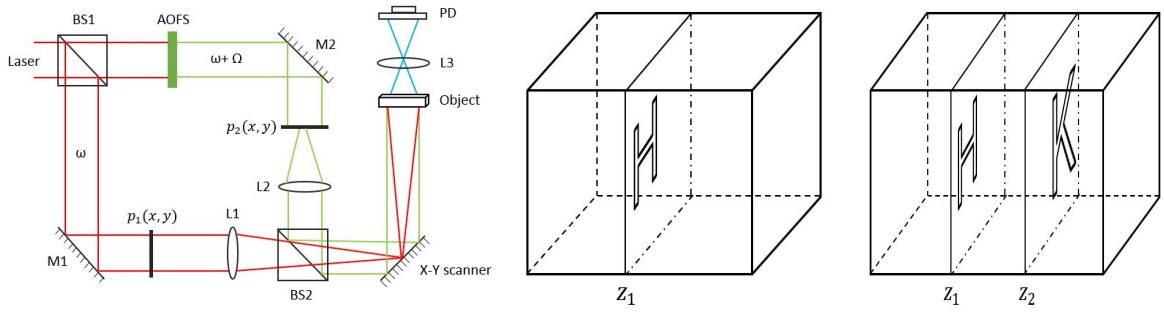

(a) (b) (c)

Fig. 1. (a) OSH system. BS1 and BS2: beam splitter; AOFS: acousto-optic frequency shifter; M1 and M2: mirror; L1, L2 and L3: lens; $p_1(x,y)$ and $p_2(x,y)$: pupil; X-Y scanner: active scanner; Object: the object to be recorded; PD: photodetector; ω and Ω: initial carrier frequency of laser and shifted frequency provided by AOFS. (b) object with one single section "H" at z_1 = 10 mm. (c) object with two sections "H" and "K" at z_1 = 10 mm and z_2 = 20 mm respectively.

Mathematically, as a two-pupil optical imaging system, when we choose the two pupils as $p_1(x,y) = 1$ and $p_2(x,y) = \delta(x,y)$, the FZP of the OSH system can be written as

$$h(x,y;z) = -j\frac{k_0}{2\pi z}\exp\left\{j\frac{k_0}{2z}(x^2+y^2)\right\}. \tag{1}$$

where $j=\sqrt{-1}$, k_0 is the wavenumber at a wavelength λ ($k_0=2\pi/\lambda$), x and y are the spatial coordinates, and z is the distance we aim to retrieve.

Suppose the object is discrete with multiple sections, specifically in our cases, the hologram $g(x,y)$ is given by

$$g_1(x,y)=|o(x,y;z_1)|^2*h(x,y;z_1), \tag{2}$$

$$g_2(x,y)=|o(x,y;z_1)|^2*h(x,y;z_1)+|o(x,y;z_2)|^2*h(x,y;z_2), \tag{3}$$

where $*$ denotes 1D convolution.

In numerical reconstruction, we convolve $h^*(x,y;z)$ with Eq. 2 and 3 to obtain the information on each section tomographically. The reconstructed image $r(x,y)$ can be written as

$$r(x,y)=g(x,y)*h^*(x,y;z). \tag{4}$$

As for one-section case, if $z=z_1$, the reconstructed image is $r(x,y)=g_1(x,y)*h^*(x,y;z_1)=|o(x,y;z_1)|^2$, which is exactly the clear and neat original object. While if $z\neq z_1$, then $r(x,y)=g_1(x,y)*h^*(x,y;z)=|o(x,y;z_1)|^2*h(x,y;z_1)*h^*(x,y;z)$. The reconstructed image will be the original object $|o(x,y;z_1)|^2$ convolutionally modulated by term $h(x,y;z_1)*h^*(x,y;z)$. The out-of-focus result may lead to the rise of fuzziness and blur of the reconstructed image. This is the same to two-section case. When $z\neq z_1$ and z_2, the reconstruction image will also become blurred. Thus we can estimate whether the reconstructed image is focused or defocused by the extent of blur and randomness.

3. Autofocusing Based on Entropy Minimization

In information theory, entropy is a measurement of how much the amount of information is included in a transmitted message; for images, entropy is often used to measure the randomness and chaos of the image values. In this paper, for the reconstructed image $r(x,y)$, we can compute the image entropy as

$$\begin{aligned} P&=\sum_{m=1}^{M}\sum_{n=1}^{N}|r(m,n)|^2,\\ p(m,n)&=\frac{|r(m,n)|^2}{P},\\ E&=-\sum_{m=1}^{M}\sum_{n=1}^{N}p(m,n)\ln p(m,n), \end{aligned} \tag{5}$$

where, for an $M\times N$ image, P is the total power of a complex image, $r(m,n)$ is the pixel value at the position (m,n) of an image, $p(m,n)$ is the ratio between the power of a pixel value and the total power, E is the entropy of this complex image.

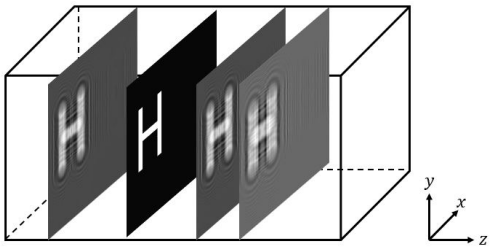

Fig. 2. For the object with one section, sequential reconstructions at 5 mm, 10 mm, 15 mm, and 18 mm. The further the reconstructed distance is away from the original position, the more chaotic and blurred the reconstructed image is.

As shown in Fig. 2, in the reconstruction, the out-of-focus effect will result in increasing the chaos of reconstructed image. The reconstruction at 15 mm is more blurred than that at 10 mm, while that at 18 mm is more blurred than that at 15 mm. Therefore entropy is an appropriate characteristic to measure the extent of chaos of the reconstructed image [7]. Concretely, we scan the z-axis within an estimated range with a certain step and calculate the corresponding entropy of each reconstructed image at a specific z. Thus we can plot a curve about entropy versus distance. At the exact position where the object locates, the reconstructed image is the clearest and neatest, which means the corresponding entropy is the smallest. Hence we can achieve the autofocusing with entropy minimization.

4. Simulation Results

To verify the effectiveness of our proposed entropy method, we conduct simulations under different situations.

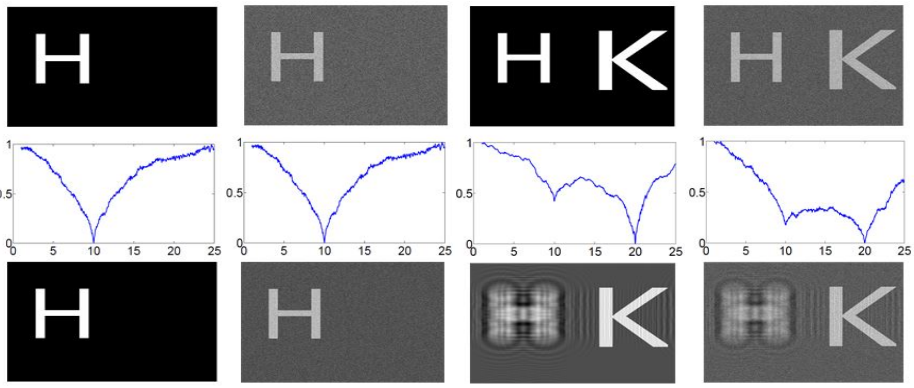

(a) (b) (c) (d)

Fig. 3. From top to bottom: (a) one section at 10 mm, the entropy curve and reconstructed image at extracted distance; (b) one section at 10 mm with random Gaussian noise located at multiple positions, the entropy curve and reconstructed image at extracted distance; (c) two sections at 10 mm and 20 mm, the entropy curve and reconstructed image at the second extracted distance; (d) two sections at 10 mm and 20 mm with random Gaussian noise located at multiple positions, the entropy curve and reconstructed image at the second extracted distance. Scanning range is from 1 mm to 25 mm. The horizontal axis is distance (unit: mm), and vertical axis is normalized entropy (unit: bit).

For the case of one single section in Fig. 3a and 3b, the entropy curves arrive at a minimum point at 10 mm, then both of them go up almost monotonously. Therefore we can assert that the section should locate at the position where the corresponding entropy is the minimum. When noise, which is modeled as random Gaussian noise image, is separately distributed along z-axis, the location of the single section can still be identified correctly.

Then we extend our method to two sections shown in Fig. 3c and 3d. Two local minimum points illustrate that there are two sections located at 10 mm and 20 mm respectively. Besides, similar to the single section case, noise does not influence the position of local minimum points either as shown in Fig. 3d.

5. Conclusion

In this paper, we use entropy as a measurement to achieve autofocusing, and verify the feasibility under different situations. The simulation results show that the proposed method can detect the distances of different sections successfully, even with the existing of noise, which is significantly conducive to reconstructing each section numerically.

Acknowledgements

This work was supported in part by the Hong Kong Research Grants Council under Projects HKU 7138/11E and 7131/12E, and by the NSFC/RGC under N_HKU714/13.

References

1. T.-C. Poon, *Optical Scanning Holography with MATLAB* (Springer-Verlag, New York, 2007), 1st ed.
2. G. Indebetouw and W. W. Zhong, "Scanning holographic microscopy of three-dimensional fluorescent specimens," Journal of the Optical Society of America A **23**, 1699–1707 (2006).
3. B. W. Schilling and G. C. Templeton, "Three-dimensional remote sensing by optical scanning holography," Applied Optics **40**, 5474–5481 (2001).
4. T. Kim and T.-C. Poon, "Autofocusing in optical scanning holography," Applied Optics **48**, H153–H159 (2009).
5. E. Y. Lam, X. Zhang, H. Vo, T.-C. Poon, and G. Indebetouw, "Three-dimensional microscopy and sectional image reconstruction using optical scanning holography," Applied Optics **48**, H113–H119 (2009).
6. X. Zhang, E. Y. Lam, T. Kim, Y. S. Kim, and T.-C. Poon, "Blind sectional image reconstruction for optical scanning holography," Optics Letters **34**, 3098–3100 (2009).
7. X. Li, G. S. Liu, and J. L. Ni, "Autofocusing of ISAR images based on entropy minimization," IEEE Transactions on Aerospace and Electronic Systems **35**, 1240–1252 (1999).